Scholar Publishing Group
Academic Journal of Energy
https://doi.org/10.38007/RE.2020.010104
ISSN 2790-2714 Vol. 1, Issue 1: 25-32

Novel Solar Cells Based on Perovskite Thin Films

Hashash Mostafa*

University of New England, Australia

**corresponding author*

Keywords: Perovskite Thin Films, New Solar Cells, Bismuth-Based Perovskites, New Energy

Abstract: The serious consumption of fossil fuels has led to many environmental problems. People have begun to seek a non-polluting new energy source to replace fossil fuels to solve the problem of energy shortage. The use of solar energy to generate electricity has become an abstract way to solve environmental pollution and energy crisis. In this paper, taking bismuth-based perovskite(BBP) as an example, a new type of solar cell prepared by using CsBi3I10 perovskite thin film avoids the toxicity of lead perovskite solar cells and is safer and more environmentally friendly. In this paper, the effect of anti-solvent and temperature on the solar performance of CsBi3I10 perovskite was investigated. It was found that when the anti-solvent low price time was 10 s, the performance parameters of solar cell devices were the largest. Increase to a certain extent, the absorption intensity will become slower.

1. Introduction

As the problem of environmental pollution caused by energy consumption becomes more and more serious, people begin to use solar energy, devote themselves to the conversion of solar energy, and develop clean energy. Among them, the development and preparation of solar cell technology is the most effective and complete way to convert solar energy into energy. In order to compete with other fossil energy sources, the production cost of solar cells(SC) must be minimized, and at the same time, higher photoelectric conversion efficiency is desired.

So far, scholars have conducted in-depth research and analysis on new types of solar cells based on perovskite thin films. For example, a scholar used spin coating method to explore the effect of electron transport material dense layer TiO_2 and mesoporous layer TiO_2 on film quality and device performance. The experiment shows that the device performance based on mesoporous TiO_2 structure is higher than that based on dense layer TiO_2 performance, can achieve a photoelectric conversion efficiency as high as 0.42% [1]. Some experimenters have prepared a Bi-based perovskite solar cell based on a bulk heterojunction. The perovskite light absorbing layer is

composed of Cs3Bi2I9 and $Ag_3Bi_2I_9$ separated in situ, and the photoelectric conversion efficiency is refreshed to 3.6%, and Voc is also obtained. A record boost to 0.89V[2]. A researcher used the gas-phase assisted solution process to expose the BiI3 film to CH_3NH_3I vapor to make the two react to prepare a $(CH_3NH_3I)_3Bi_2I_9$ perovskite film with a smooth, uniform surface and high morphological quality. Titanite solar cells have the highest PCE and high repeatability [3]. A certain scholar added TFEACl to inhibit the segregation of SnF_2, which improved the morphology of the film in addition to more favorable band alignment and improved inhibition of Sn4+ formation. The reduced charge recombination and improved charge collection lead to enhanced efficiency and significantly improved stability of SC devices [4]. Although the research results on the preparation of SC from perovskite thin films are good, these new SC need to ensure good stability and non-toxicity before they can be widely used.

This paper first introduces the source of bismuth-based perovskite SC, then begins to use perovskite to prepare SC, analyzes the preparation process and raw materials of various structures of SC, and finally studies the performance of the perovskite SC prepared in this paper. The effects of anti-solvent addition time and temperature changes on battery performance during the preparation process were analyzed.

2. Overview of Solar Cells

2.1. New Perovskite Solar Cells

(1) New solar cells

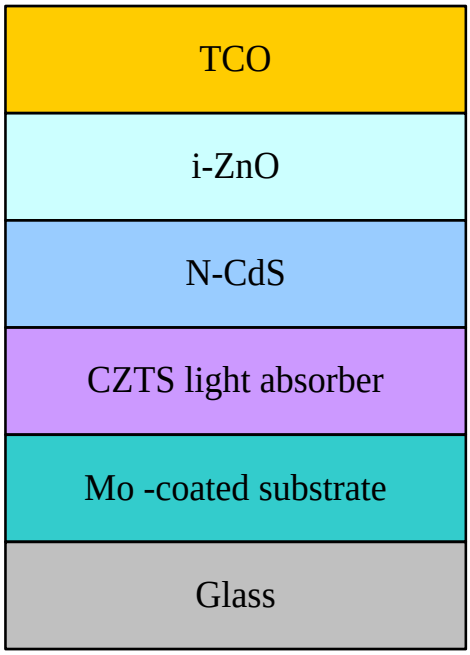

Figure 1. Schematic diagram of CZTS photovoltaic device

CZTS has attracted much attention due to its application in high-density photovoltaic thin films. The diagram of the CZTS photovoltaic device is shown in Figure 1. CZTS thin film solar cells are small in size and rich in zinc and tin, which greatly reduces the cost and is considered to expand the scope of use [5]. In addition, as an important compound thin film absorbing material, CZTS has

better optical properties and suitable coupling frequency. Concerns about the cost and availability of indium in CIGS and the acidity of tellurium in CdTe and cadmium are important factors to study other oxidative stress factors [6-7].

(2) BBP solar cells

Lead perovskites achieve the highest-performing solution-processed solar cells ever, rivaling the efficiency of commercial crystalline silicon solar cells. But lead toxicity interferes with the functioning of the blood, kidneys, liver, brain, and nervous system [8]. The toxicity issue of lead has prompted some researchers to look for alternatives to lead-based perovskites, also known as BBP. BBP materials are candidates for non-lead perovskite solar cell applications because of their non-toxicity and high stability in air [9].

2.2. Perovskite Solar Cell Structure

(1) Electron transport layer

Improving the PCE of perovskite solar cells by increasing electron mobility, suggesting the criticality of facilitating charge dissociation/transport through bulk transport of fullerenes. Fullerenes by themselves cannot fully form perfect ohmic contacts with metals such as Al or Ag [10].

(2) Hole transport layer(HTL)

HTL can be divided into three categories: inorganic, polymeric and small molecules [11]. The HTM layer and the perovskite layer are in close contact. It is always necessary to use HTM to remove the holes on the perovskite and direct them to the electrodes. The most common HTM is Spiro-OMeTAD, which is the most widely studied HTM for solid-state sensitized solar cells in the past two decades. At the same time, 70 kinds of conjugated conductive polymers were developed as PSC organic HTMs [12-13].

2.3. Performance Parameters of Solar Cells

In most cases, when testing the performance of solar cells and their components, a constant natural light source or a simulated light source AM1.5 is used. The counter electrode is often used in solar cell devices, which results in a certain common function difference. The internal and external quantum efficiency of the cell can be expressed as EQE, which is another important parameter of solar cells) [14]. Since the cell cannot completely absorb the incident photons, the internal quantum efficiency(IQE) is often larger than the corresponding IQE. v_{oc} is the voltage value when the SC is in the open-circuit state, that is, the current is 0, under the condition of natural light source or standard simulated light source [15].

$$Y = \frac{P_{\max}}{v_{oc} \times I_{sc}} \tag{1}$$

Among them, $P_{\max}$ is the maximum power, I_{sc} is the short-circuit current of the theoretical output power, v_{oc} is the open-circuit voltage(OCV), and Y is a constant less than 1. The influence of other conditions is not considered. In theory, the larger the Y, the better the battery performance.

$$\eta_s(\%) = \frac{P_{max}}{P_{in}} \times 100\% \quad (2)$$

where η is the photoelectric conversion efficiency of the battery, and P_{in} is the incident power of sunlight. Transparent electrodes and metal electrodes are mainly used in perovskite solar cells, which are mainly used to collect charges, and the electrodes are used to collect holes. The light transmittance of FTO is basically the same as that of ito. Compared with FTO, ito is a heavily doped n-type semiconductor with a high work function bandgap of 3.7ev, high transmittance (above 80%) in the visible region, and high conductivity [16].

3. Perovskite Thin Films to Prepare New Solar Cells

3.1. Preparation of Perovskite Film

The perovskite light-absorbing layer was prepared by a one-step spin coating method: 453.6 mg of BiI_2 and 272.8 mg of CsI (the molar ratio of BiI_2 and CsI was 2:3) were dissolved in 800 μL DMF and 200 μL DMSO (v:v=4: 1) In the mixed solvent of 1), weigh 461.4 mg of BiI2 and 71.5 mg of CsI (the molar ratio of BiI_2 and CsI is 3:1) and dissolve them in a mixed solvent of 800 μL DMF and 200 μL DMSO (v:v=4:1) , and stirred overnight at 70 ℃ to form a $Cs_3Bi_2I_9$ precursor solution and a $CsBi_3I_{10}$ precursor solution, respectively. Take 60 μL of bismuth-based perovskite precursor solution and coat it on the surface of SnO_2 film.

3.2. Preparation of Hole Transport Layer

A NiOx precursor solution was obtained by dissolving 248.8 mg $Ni(CH_3COO)_2*4H_2O$ in 10 mL ethanol (0 proof grade) with 60 uL ethanolamine and stirring at 60 ℃ for 40 minutes. Use a pipette to take 100 μL of the precursor solution and drop it on the ITO glass, spin it at 2000 rpm for 40 seconds, and place it on a 300 ℃ hot stage. UV-ozone treatment [18].

3.3. Preparation of Perovskite Absorber Layer

The deposition of perovskite films was performed in an N_2 glove box. The perovskite films treated with CB were fabricated by dropwise addition of chlorobenzene solvent within 10 s of the spin coating process and subjected to the same annealing process.

3.4. Device Preparation

The TiO_2 was cleaned with ethanol, treated with oxygen plasma, and then spin-coated to form an electron transport layer, and finally annealed at 500C for 30 minutes. The mesoporous TiO_2 layer was spin-coated with commercially available TiO_2. The substrate was baked at 500C for 30 minutes before the perovskite layer was deposited on the substrate. The PbI_2 precursor solution is obtained by incorporating PbI_2 powder into DMF, DMSO and their mixtures (mixing ratio 1:1), with a mass fraction of 20% [19]. Inkjet printing includes a motorized x-, y-, and z-direction piezoelectrically driven inkjet head. The mesoporous TiO_2 substrate was placed on the platen at a relative humidity of 40% and a temperature of 50 ℃ in the printing chamber. After PbI_2 deposition, the samples were

transferred to a glove box containing N_2 for annealing for two hours, and the MAI powder was deposited on PbI_2 to generate perovskites by in situ reaction. Finally, 90nm-thick gold was deposited on the surface of the track by thermal evaporation under a vacuum pressure of 3x10-5 Torr [20].

4. Experimental Analysis

4.1. The Effect of Antisolvent on the Performance of Perovskite SC

Table 1. Solar cell device performance with different antisolvent treatment times

time (s)	Voc(V)	Jsc(mA/cm^2)	Y(%)	PCE(%)
0	0.49	1.05	45.64	0.27
5	0.46	1.64	47.39	0.31
10	0.45	1.82	48.21	0.38
15	0.46	0.93	46.07	0.14

Table 1 shows the relevant device performance parameters of $CsBi_3I_{10}$ solar cells under different anti-solvent treatment times. It can be seen from the table that when no anti-solvent treatment is performed, the best photoelectric conversion efficiency of $CsBi_3I_{10}$ perovskite SC is 0.27%, among which , the values of Voc, Jsc, and Y are 0.49V, 1.05mA/cm2, and 45.64%, respectively. When the anti-solvent dripping time was 10s, the optimal PCE value of the device increased to 0.38%, the corresponding Voc, Jsc, Y were 0.45V, 1.82mA/cm2, 48.21%, and the PCE was 0.38%. Comparing the performance parameters of the two, we found that the increase in the Jsc value is the most obvious, and it is relevant to obtain the highest film morphology quality and the highest light absorption after the anti-solvent addition time is optimized.

Table 2. Absorption intensities (%) of perovskite films prepared with different chlorobenzene dropping times

time (s)	200	300	400	500	600	700	800
0	63.5	60.2	58.7	36.9	24.8	13.6	9.4
5	76.4	72.5	59.3	38.2	24.3	12.7	9.3
10	91.6	83.7	72.4	37.5	25.8	13.2	10.1
15	89.7	82.5	68.6	33.8	21.4	11.5	9.2

Table 2 is the UV-vis absorption spectrum of $CsBi_3I_{10}$ thin film under different chlorobenzene dropping time. Because the concentration of the perovskite precursor is fixed under different conditions, the spin coating parameters and the annealing temperature are also fixed, and the thickness of the prepared perovskite films is similar, so the difference in the absorption spectrum of each film is mainly affected by the surface morphology of the film. influence on appearance quality. When no chlorobenzene treatment is performed, a large number of holes appear on the surface of the film, which makes the film have weak absorption intensity; when the anti-solvent chlorobenzene is added dropwise for 10s, the perovskite film is in the visible light range with a wavelength of 400-700 nm. There is a high absorption intensity, and the characteristic absorption sideband of perovskite $CsBi_3I_{10}$ appears at the wavelength of about 700nm, which is due to the higher quality of the film under the condition of dropping anti-solvent in the 10s, so the corresponding However, when the anti-solvent chlorobenzene was added dropwise at 15s, the absorption intensity of the film was lower than that of the film without chlorobenzene treatment. At this time, the surface of the

film had the most holes and the worst flatness. Rough films will cause severe light scattering, which can mask or even suppress the intrinsic absorption of perovskite films. To sum up, too early or too late addition time of anti-solvent chlorobenzene will affect the light absorption performance of $CsBi_3I_{10}$ film, and the optimal addition time of chlorobenzene is 10s , and the perovskite film prepared under this condition has the strongest light absorption ability.

4.2. The Effect of Temperature on Perovskite Solar Cells

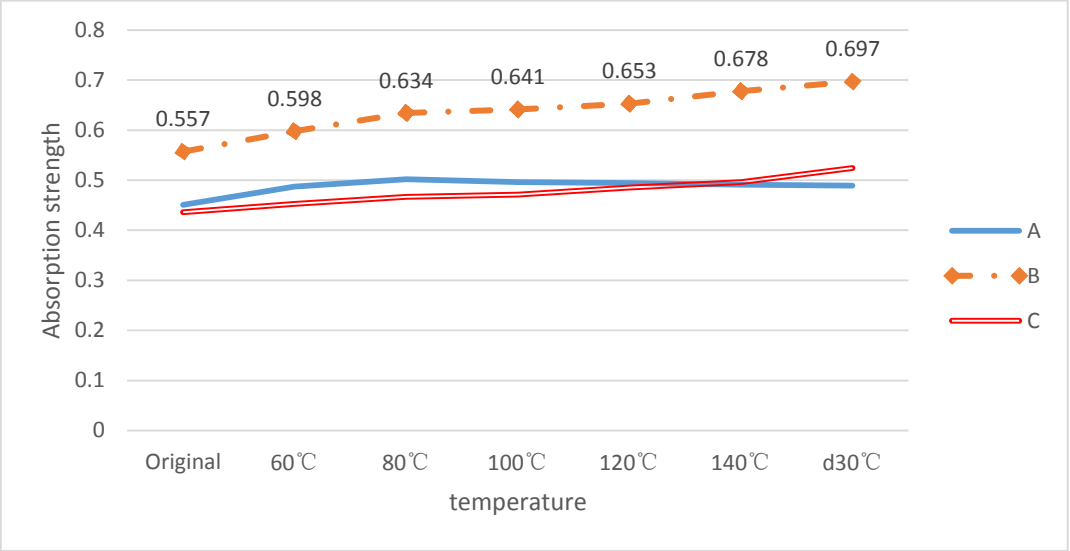

Figure 2. λ=300nm thin film UV-Vis absorption intensity

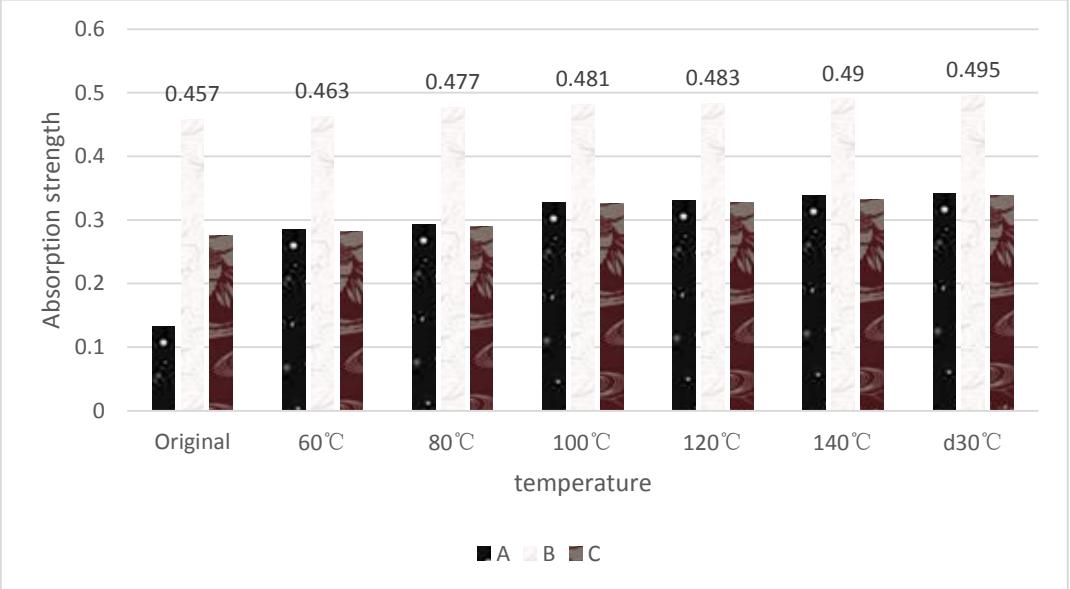

Figure 3. λ=600nm thin film UV-Vis absorption intensity

Comparing the absorption intensities of films near λ=300nm and λ=600nm at different temperatures, as shown in Figure 2 and Figure 3, the UV-Vis absorption intensities of perovskite

films near λ=300nm and λ=600nm at various temperatures, respectively Comparison of specific values. The absorption intensities of the three film samples A, B, and C at 300 nm and 600 nm were compared in turn at each temperature. As the temperature increased, the absorptions of the three films at 300 nm and 600 nm were significantly enhanced, and there was still enhancement after 100 ℃. But it is very slow. When the temperature drops to 30 ℃, the absorption strength of some films even decreases slightly. It can be seen that when the temperature rises to 100 ℃, the absorption intensity increases slowly, and the spectrum almost no longer changes significantly. The influence of temperature on the absorption strength of the film is mainly due to the influence of the growth rate of the film at a certain temperature and the change of the grain size.

5. Conclusion

Due to the increasing consumption of fossil energy and worsening air pollution, there is an urgent need to provide clean and renewable energy resources for mankind. Among new energy solutions, photovoltaic (PV) technology, which converts solar energy directly into electricity, is a promising approach to safely obtain sustainable and clean energy. In this paper, new-energy SC are prepared by using BBP thin films. In the research of $CsBi_3I_{10}$ perovskite SC, the photoelectric conversion efficiency of SC can be improved by optimizing the dripping time of anti-solvent. The absorption spectrum of $CsBi_3I_{10}$ perovskite material is wider than that of $CsBi_3I_9$ perovskite material, which is beneficial to improve the photocurrent of perovskite SC.

Funding

This article is not supported by any foundation.

Data Availability

Data sharing is not applicable to this article as no new data were created or analysed in this study.

Conflict of Interest

The author states that this article has no conflict of interest.

References

[1] Jo Y R , Koo B , Seo M J , et al. Growth Kinetics of Individual Co Particles Ex-solved on SrTi_(0.75)Co_(0.25)O_(3-δ) Polycrystalline Perovskite Thin Films. Journal of the American Chemical Society, 2019, 141(16):6690-6697.

[2] Lim J , Horantner M T , Sakai N , et al. Elucidating the long-range charge carrier mobility in metal halide perovskite thin films. Energy & Environmental ence, 2018, 12(1):169-176.

[3] Khudyakov D V , Ganin D V , Lyashedko A D , et al. Nonlinear optical absorption in thin halide perovskite films under femtosecond excitation at wavelengths of 1064 and 532 nm. Quantum Electronics, 2020, 51(3):211-216. https://doi.org/10.1070/QEL17494

[4] Bonomo M , Carlo A D , Centore R , et al. New pyran-based dyes as efficient sensitizers of p-type dye-sensitized solar cells. Solar Energy, 2018, 169(jul.):237-241.

[5] Kumaran T S , Prakasam A , Anbarasan P M , et al. New Phenoxazine-Based Organic Dyes

with Various Acceptors for Dye-Sensitized Solar Cells: Synthesis, Characterization, DSSCs Fabrications and DFT Study. Journal of Computational Biophysics and Chemistry, 2020, 20(05):465-476. https://doi.org/10.1142/S2737416521500253

[6] Yusupov, A. Electric Properties of p-Cu2ZnSn(S_(1-x)Se_x)_4/n-Si Heterojunctions for The Creation New of Solar Cells. Acta of Turin Polytechnic University in Tashkent, 2019, 9(2):6-6.

[7] Abdellatif S O , Josten S , Khalil A , et al. Transparency and Diffused Light Efficiency of Dye-Sensitized Solar Cells: Tuning and a New Figure of Merit. IEEE Journal of Photovoltaics, 2020, 10(2):522-530. https://doi.org/10.1109/JPHOTOV.2020.2965399

[8] Ravi V K , Mondal B , Nawale V V , et al. Don't Let the Lead Out : New Material Chemistry Approaches for Sustainable Lead Halide Perovskite Solar Cells. ACS Omega, 2020, 5(46):29631-29641. https://doi.org/10.1021/acsomega.0c04599

[9] Nehme V , Nehme M , Ghaddar T H . New pyridyl-based dyes for co-sensitization in dye sensitized solar cells. Solar Energy, 2019, 187(JUL.):108-114.

[10] Kumar S S , Vairam S , Neelakandeswari N , et al. New heterojunction solar cells using copper oxide ingrained MWCNT: Fabrication and performance analysis. Solar Energy, 2018, 166(MAY):195-202.

[11] Kokal R K , Bhattacharya S , Cardoso L S , et al. Low cost 'green' dye sensitized solar cells based on New Fuchsin dye with aqueous electrolyte and platinum-free counter electrodes. Solar Energy, 2019, 188(AUG.):913-923.

[12] Rajan A K , Cindrella L . Studies on new natural dye sensitizers from Indigofera tinctoria in dye-sensitized solar cells. Optical Materials, 2019, 88(FEB.):39-47.

[13] Tak S , Tarkas H , Bisen G , et al. A new approach for preparation of ternary bulk-heterojunction using dual- feed ultrasonic spray for organic solar cells. Optical Materials, 2019, 91(MAY):296-304.

[14] Jagadamma L K , Taylor R , Kanibolotsky A L , et al. Highly efficient fullerene and non-fullerene based ternary organic solar cells incorporating a new tetrathiocin-cored semiconductor. Sustainable Energy & Fuels, 2019, 3(8):2087-2099. https://doi.org/10.1039/C9SE00343F

[15] R, Kacimi, T, et al. New organic molecular based on Bis-Dipolar Diphenylamino-EndcappedOligo Aryl Fluorene Application for organic solar cells - ScienceDirect. Materials Today: Proceedings, 2019, 13(Part 3):1178-1187.

[16] Pourandarjani A , Nasirpouri F . A new approach to understanding the deficiency of backside illuminated dye-sensitized solar cells' fill factor as a result of cracking of the TNAs. Materials Today: Proceedings, 2019, 18(Part 2):501-509.

[17] Tamilavan, Vellaiappillai, Liu, et al. Highly crystalline new benzodithiophene-benzothiadiazole copolymer for efficient ternary polymer solar cells with an energy conversion efficiency of over 10%. Journal of Materials Chemistry, C. materials for optical and electronic devices, 2018, 6(15):4281-4289. https://doi.org/10.1039/C8TC00817E

[18] Mbarek M , Sagaama L , Alimi K . New copolymer involving PVK and F8BT for organic solar cells applications: Design, synthesis, characterization and theoretical studies. Optical Materials, 2019, 91(MAY):447-454.

[19] Beni, Ali, Reza, et al. New organic dyes with diphenylamine core for dye-sensitized solar cells. Journal of Materials Science. Materials in Electronics, 2018, 29(8):6323-6336.

[20] Mondal A , Bandyopadhyay S , Mondal A K , et al. Evaluation of New Acid Composition for Low Optical Reflectance Texturization of Multicrystalline Silicon Wafer for Solar Cells. IEEE Journal of Photovoltaics, 2019, 9(4):951-956. https://doi.org/10.1109/JPHOTOV.2019.2911111